Reviews on Advanced Materials and Technologies, 2026, vol. 8, no. 2, pp. 125–134
DOI: 10.17586/2687-0568-2026-8-2-125-134

Polydimethylsiloxane Thermal Insulation Composite Elastomer Filled with Hollow Glass Microspheres

E.V. Antonov [1,*], D. Castro [2], P.P. Snetkov [1], S.N. Morozkina [1,3], I.M. Sosnin [1,4], L.M. Dorogin [1]

[1] Institute for Advanced Data Transmission Systems, ITMO University, Kronverkskiy pr., 49, lit. A, St. Petersburg, 197101, Russia
[2] Center for Chemical Engineering, ITMO University, Kronverkskiy pr., 49, lit. A, St. Petersburg, 197101, Russia
[3] Kabardino-Balkarian State University, Chernyshevskogo str, 174, Nalchik, Russia
[4] Togliatti State University, Belorusskaya str., 14, Togliatti, 445020, Russia

Article history

Received May 15, 2026
Received in revised form, June 26, 2026
Accepted June 29, 2026
Available online June 30, 2026

Abstract

This study aims to enhance the thermal insulation properties of polydimethylsiloxane by the incorporation of hollow glass microspheres (HGM) as a functional filler, while evaluating the trade-offs in mechanical, surface, and optical performance. The thermal conductivity, tensile mechanical properties, surface characteristics, and optical transparency of the composites were investigated. The incorporation of 10 wt.% hollow glass microspheres decreased the thermal conductivity coefficient by 56.3%, achieving a minimum value of 0.059 $W \cdot m^{-1} \cdot K^{-1}$. However, this enhancement came at the expense of optical transparency, surface properties, and a significant reduction in the critical elongation at the break. The results demonstrate that HGM-filled polydimethylsiloxane composites are promising materials for thermal insulation applications where transparency and stretchability are secondary to thermal performance.

Keywords: Thermal conductivity; Microspheres; Adhesion; Polydimethylsiloxane; Composite material

1. INTRODUCTION

The problem of thermal management in modern electronics stimulates the development of localized heat flow control. The application of advanced thermal insulation materials may lead to a reduction in both the parasitic thermal leakage within multilayered printed circuit boards – achieved by minimizing cross-talk between adjacent thermal zones and the cooling energy consumption of electronics devices, thereby enhancing overall performance and lifespan. This is quite important in several applications, such as aerospace avionics [1,2], portable consumer electronics [3–5], automotive power controllers [6]. In this direction, beside thermal insulation, mechanical properties are quite important; as well as environmental and toxic safety, thermal and chemical stability.

Thermal insulation materials, which serve as one of the primary means of controlling heat transfer, are the subject of extensive research and are critically important for advancement in this field. Obtaining porous materials (for example, based on foam or aerogel) is the most priority direction of thermal insulation materials fabrication [7–10]. In the article [11] magnesium oxychloride cement with halloysite-based aerogels and hydroxy-terminated polydimethylsiloxane were fabricated. In the work of Chong et. al. [12] the material with fiberglass and mineral wood was developed. The development of organic thermal insulators is more widely represented. Materials based on paraffin with passive thermal regulations are described in the work of Guo and Feng [13], the fabrication of a cotton linter celluloses composite with a sponge structure for an insole is presented in the article [14], and there are other developments highlighted [15,16]. Several studies also take into account the fabrication of thermal insulators based on classical polymers [17], or the silicon aerogels [9,18,19]. However, many polymers used in thermal insulation materials have limitations because of their flammability, susceptibility to water and chemicals, and unsatisfactory mechanical properties.

One of the most widely used polymers in advanced applications is polydimethylsiloxane (PDMS). It serves as a foundational material in microfluidics for lab-

* Corresponding author: E.V. Antonov, e-mail: evantonov@itmo.ru

© 2026 ITMO University. This is an open access article under the terms of the CC BY-NC 4.0 license.

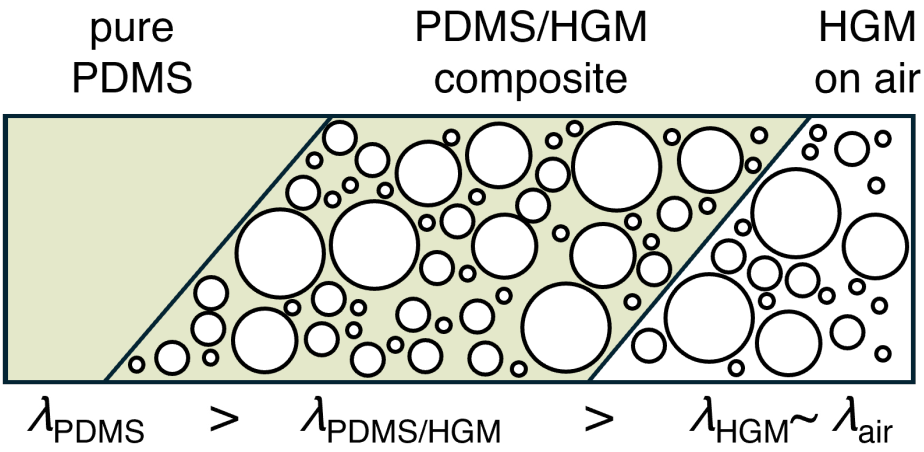

Fig. 1. PDMS/HGM composite (center) with the controlled pore-similar air gap and thermal conductivity coefficient $\lambda_{PDMS/HGM}$ can be obtained by the introduction of a HGM filler (right) into pristine PDMS elastomer (left).

on-a-chip devices, in wearable technology for flexible electronics [20], and in medicine for implantable systems [21], soft robotics [22], photocatalytic applications [23,24] and energy harvesting. It has the advantage due to relatively low wettability and thermal, electrical conductivity, thermal and chemical stability, mechanical and surface properties, and processability of manufacturing [25–28]. When compared to common polymeric thermal insulators such as polystyrene or polyurethane foams, PDMS exhibits exceptional thermal stability, maintaining its properties in a wide temperature range (–60 °C to +200 °C) [29]. PDMS is also actively used in the development of thermal insulation materials [30,31]. Many efforts have been done to develop modification of PDMS for achieving of foam, aerogels or increase porosity [32–35]. Several authors fabricated the foamed materials [11,17,36]. While the porosity discussed in the aforementioned studies (i.e., a high density of internal air gaps) is highly effective at reducing thermal conductivity, it concurrently leads to detrimental changes in mechanical strength, surface characteristics, and material cohesion. Furthermore, achieving such porosity often requires complex and challenging manufacturing techniques. These changes of mechanical properties may make foam insulation unsuitable for specialized applications where mechanical resilience and performance under thermal cycling are essential, as aerospace components [2], protective thermal management systems in electric vehicle batteries where thermal runaway protection is critical [6], and as conformal insulation for wearable high-temperature protective equipment [4].

Hollow glass microsphere (HGM), as a filler, can be efficient for the production of thermal insulation materials [37,38]. HGM is low-cost, compressive high-strength, low thermal conductivity due to hollow (Fig. 1). Furthermore, the production of composite materials based on PDMS with this filler requires minimal change of the fabrication technology in the comparison to original PDMS preparation [15,39]. Unlike solid ceramics like Al_2O_3 or SiO_2, which increase both density and thermal conductivity, HGM simultaneously reduces weight and heat transfer, while offering simpler processing and greater mechanical robustness than fragile aerogels. This positions HGM as a practical solution for creating lightweight, efficient thermal insulators where ease of fabrication and durability are critical. While the initial material cost of PDMS-based composites with hollow glass microspheres is higher than conventional polymer insulators like expanded polystyrene or polyurethane foams, their economic benefits include: extended service life due to exceptional resistance to environmental degradation (moisture, UV radiation, temperature cycling); reduced maintenance costs as PDMS/HGM composites maintain their insulating properties without deterioration over time; energy efficiency savings in high-temperature applications where traditional foams would degrade rapidly; and installation advantages for complex geometries due to their flexibility and form-fitting properties.

In the present work we fabricated the composite materials based on PDMS-matrix with the content of HGM as the filler from 0 to 10 wt.%. for thermal insulation application. The production process used the mixer for the agitation of the solution; curing was carried out in a muffle furnace with rotation of the materials during the process. The thermophysical, surface, optical and mechanical properties of the fabricated composites were studied, and SEM-images were obtained for the analysis of the distribution and the shells safeness of the filler in materials. It has to be noted, that composite materials based on PDMS with HGM-filler have been recently developed and studied in our group [40], but in this work we used HGM obtained from other manufacturer and used the mix-

ing method. Similar work was also performed in Ref. [41], however, in our work, the commercial silgard 184 kit was used as a PDMS.

2. MATERIALS AND METHODS

2.1. Materials preparation

Sylgard 184 from Dow Corning (USA), as a PDMS, with proportion curing to the base agents 10 to 1 was used for the fabrication of composite materials. HGM from GraphitePRO (Russia), with bulk density of 0.19 g·cm^{-3} and mean size 65 μm in concentration from 0 to 10 wt.% were used as the filler. The obtained solution was mixed for 5 minutes at 3500 rpm using SpeedMixer™ DAC 150.1 FVZ 5 (Germany). The uniformly mixed solution was then cast into a 12×12×3 mm polytetrafluoroethylene (PTFE) mold, degassed at ~30 kPa, sealed, and thermally cured at 140 °C for 2 h in a muffle furnace. The size of the cured material was 12×12×0.3 cm, but for the study of the properties, a material of 10×10×0.3 cm in size was cut from the center to avoid anomalies at the edges. Thus, the volume of the final material was kept constant, independent of the initial solution mass. Samples with six different concentrations of HGM were prepared. The mass of the obtained samples decreases from 33 g at 0 wt.% HGM to 20 g at 10 wt.% HGM (by 1.65 times), which is a consequence of the filler's low density.

Analogous mixtures were prepared in Petri dishes and subjected to the room-temperature curing (thus, omitting the thermal treatment in a muffle furnace) for other analytical techniques. The thermal, optical, mechanical and surface properties of the samples were characterized.

2.2. Scanning electron microscopy image

To study the distribution of filler in the material (PDMS), its safeness, as well as the HGM size the scanning electron microscope (SEM) Tescan MIRA-3 with high brightness Schottky cathode was used. The samples were pre-coated with a 10 nm thick gold layer, the working distance was ~25 mm, and the accelerating voltage (SEM-HV) was 15 kV. SEM-image of the top, bottom surface, and cross section after the fracture of samples with 10 wt.% HGM concentration were obtained.

2.3. Thermal conductivity measurement

Thermal conductivity was measured using ITP-MG4 device (Stroypribor, Russia) by the method of stationary heat flow with samples 10×10×0.3 cm. The experiment was carried out for 20 minutes with the temperature of the hot edge T_H = 30 °C and the temperature of the cooler T_R = 15 °C (the temperature gradient is ΔT = 15 °C), and with the pressure on the sample of 2.5 kPa (the error is < 2.5%). Each sample was measured at least 3 times.

2.4. Mechanical properties

For the study of mechanical properties, the elongation at the break was measured using strength testing machine INSTRON 5966 (USA). The speed of deformation was 70 mm/min. Each sample was divided into five 10×1 cm sections. Measurements were performed uniformly across all sections in accordance with ISO 527-2:2012, utilizing a Type 3 specimen.

2.5. Optical properties

Optical properties obtained materials were investigated using a Lambda 1050 spectrophotometer (PerkinElmer, Waltham, Massachusetts, USA). Reflectance spectra were recorded in the range of 250–2500 nm for the original PDMS elastomer (in the mold and in the Petri dish), as well as for samples with a HGM content of 2.5%, 5%, and 10%. Instead of analyzing the transmission spectra, the reflection spectra analysis method was chosen because the sample with HGM filler lost its optical transparency (at a thickness of about 3 mm).

2.6. Surface properties

Surface properties of the samples prepared in Petri dishes were studied by the measuring of adhesion work to glass and water wettability.

The adhesion work of the sample to glass probe was studied by the using of the experimental setup based on the Johnson-Kendell-Roberts model (JKR-model) [42], with the probe descent speed of $4.68 \cdot 10^{-5}$ m·sec^{-1}, cycle distance 0.01995 m, radius of 1.25 cm, and contact delay 2 seconds and load 6–7 grams (values on the scales). Before each experiment the glass probe was anti-dust treated.

The water wettability of the sample prepared in Petri dishes was measured for pristine PDMS and for the sample with 10 wt.% HGM by the method of sessile drop. We fixed the contact angle (advancing) of drop of liquid (water) right after the application and in 8 minutes (receding) by digital microscope (Dino-Lite Edge Digital Microscope, China). Then the equilibrium contact angle was calculated using the equation as it described in the work [43].

3. RESULTS

3.1. Samples preparation

Surface roughness of the samples increased with higher HGM concentration. Furthermore, the curing process was

Table 1. Characterization of the samples.

Sample	Microsphere content, %	λ, $W \cdot m^{-1} \cdot K^{-1}$	R, $m^2 \cdot K \cdot W^{-1}$	Thickness, mm
PDMS/HGM-0	0	0.136 ± 0.001	0.023 ± 0.001	3.2 ± 0.2
PDMS/HGM-1	1.0	0.113 ± 0.003	0.030 ± 0.001	3.1 ± 0.3
PDMS/HGM-2	2.5	0.082 ± 0.004	0.036 ± 0.003	3.0 ± 0.3
PDMS/HGM-5	5	0.075 ± 0.002	0.043 ± 0.001	3.2 ± 0.2
PDMS/HGM-7	7.5	0.069 ± 0.002	0.047 ± 0.001	3.0 ± 0.2
PDMS/HGM-10	10	0.059 ± 0.001	0.050 ± 0.001	3.0 ± 0.2

accelerated at higher HGM loadings. The samples prepared in Petri dishes, with the exception of the 0% and 10% HGM compositions, exhibited pronounced sedimentation. This occurred due to the absence of a thermal crosslinking catalyst, which resulted in an excessively long curing process. During this prolonged period, the HGMs sedimented as a result of the significant density mismatch between the HGMs and the PDMS matrix.

It is noteworthy that the pristine PDMS elastomer samples fabricated in a Teflon mold exhibited significantly reduced optical transparency compared to their counterparts prepared in Petri dishes. This phenomenon is attributed to the combined effects of interfacial stress-induced surface microtopography and localized cross-linking heterogeneity. The ultra-low surface energy of PTFE promotes cohesive failure within the PDMS near the interface during demolding, generating light-scattering surface defects absent in samples from higher-energy polystyrene surfaces. However, analysis of the optical properties did not reveal any significant differences. In addition, the samples prepared in Teflon's mold had increased visually roughness. At the time, the samples with filler and prepared in the mold, had smoother surface than the similar samples prepared in Petri dishes.

The obtained samples have different thicknesses, regardless of the mold used, although the average thickness of the material did not change significantly (Table 1).

In contrast to our previous study [40], where ultrasonic bath treatment combined with manual stirring ensured uniform filler dispersion, the current work employs mechanical mixer agitation. This method, while efficient for large-scale processing, introduces significant shear forces that lead to heterogeneous HGM distribution, increased air entrapment requiring extended degassing, and potential fragmentation of hollow microspheres. These factors collectively contribute to the observed higher data scatter in tensile properties and reduced effectiveness in thermal conductivity reduction per unit filler content. Furthermore, it is critical to note that HGM properties vary considerably between suppliers due to differences in glass composition, wall thickness uniformity, and particle size distribution. Such variability necessitates careful supplier selection and thorough characterization of filler properties to ensure reproducibility and optimal material performance in polymer composites.

3.2. SEM image

The compositions based on HGM-filler were investigated by SEM analysis. According to the data presented in Fig. 2, the uniform distribution of the HGM-filler composition did not reach. The surfaces of top and bottom sides have significant difference in quantity of HGM with the resulting from this roughness, gaps (breaks), safeness of HGM-shell and volume content of PDMS. As it is demonstrated in Fig. 2b, the break of HGM after composite curing does not lead to the decrease of thermal conductivity. This can be explained by the fact that a pore remains at the site of the HGM's destruction. The wall thickness of HGM was found to be approximately 1–2 μm. For correctness, it is necessary to calculate the proportions of destruction of microspheres with an increase in their total content in the material, which will be done in further study.

3.3. Results of thermal conductivity measurement

The dependence of the thermal conductivity (TC) of PDMS-based composite materials on the concentration of HGM is shown in Fig. 3. It has to be noted that TC of the obtained PDMS without HGM is lower than stated by the manufacturer (0.27 $W \cdot m^{-1} \cdot K^{-1}$). It can be achieved by the degassing procedure, that deletes air from the material. The thermal conductivity of composite materials based on PDMS is inversely proportional to HGM content in composite. The Pearson correlation coefficient (a statistical measure of the linear relationship between two variables) is –0.895, which indicates a strong inverse relationship between thermal conductivity and HGM content. The thermal conductivity with 10% HGM content is 0.059 $W \cdot m^{-1} \cdot K^{-1}$, that is 43.7% of pristine PDMS thermal conductivity. Also, with 2.5% HGM the thermal conductivity decreased by 40%. At higher HGM concentrations, increased inter-particle contact during mixing leads to filler abrasion and destruction. This may explain why a more effective reduction in thermal conductivity is observed at lower filler loadings.

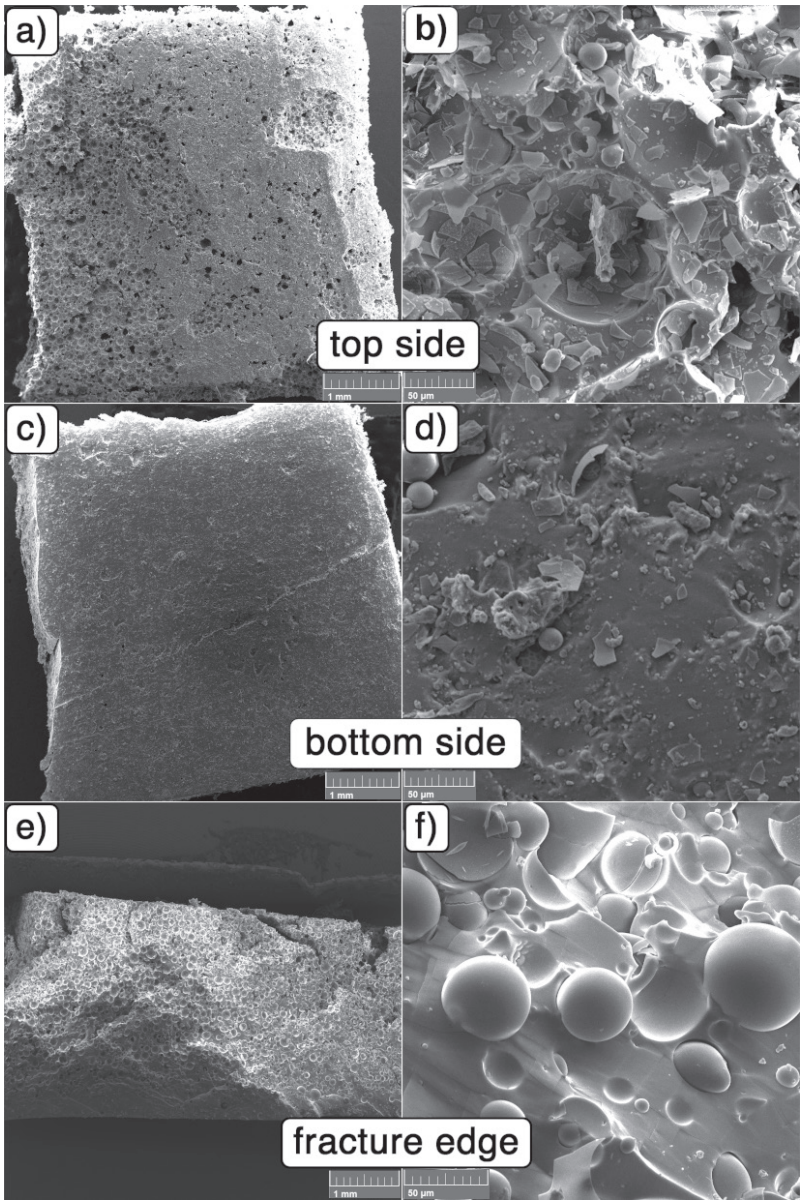

Fig. 2. SEM images of PDMS/HGM-10 composite samples at the scale of 1 mm (left) and 50 μm (right): (a,b) and (c,d) are images of the top and bottom surfaces of the composite, respectively, to study the uniformity of distribution; (e) and (f) are the cross section obtained by fracture, to preserve microspheres in order to analyze their integrity in the volume of the material.

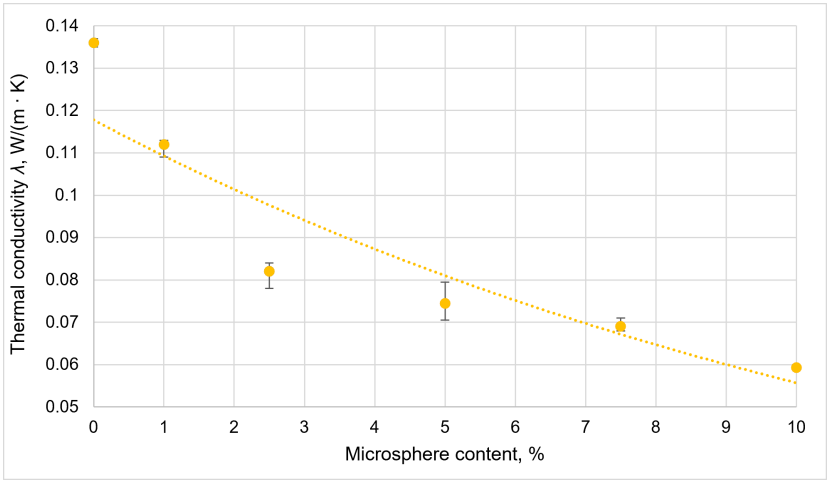

Fig. 3. The dependence of thermal conductivity of PDMS composite on HGM content.

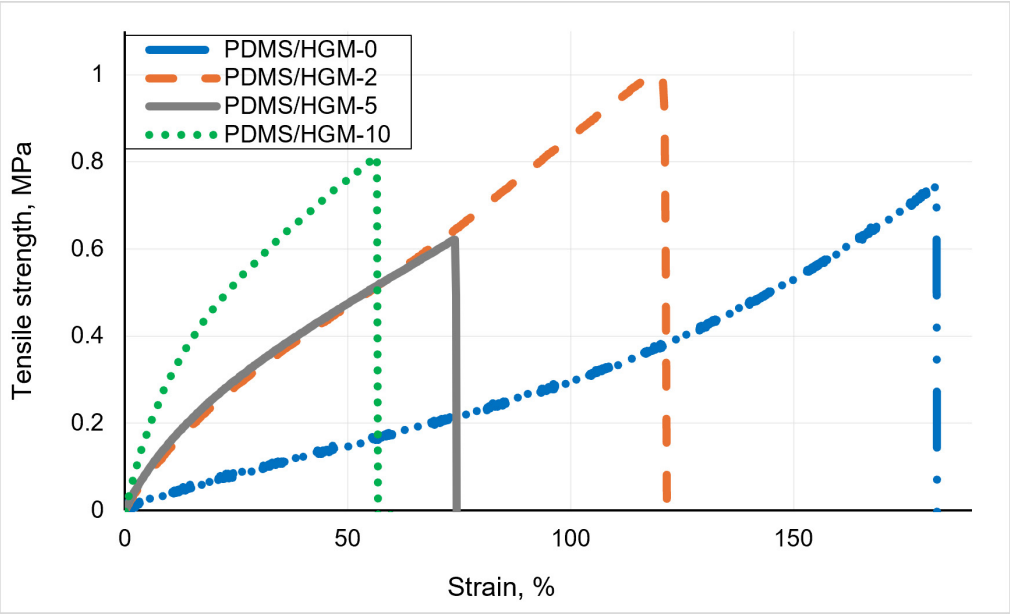

Fig. 4. The curves of the deformation-stress for the samples with different HGM content. The blue dash-dotted, orange dashed, solid grey and green dotted curves correspond to the samples with 0%, 2.5%, 5% and 10% HGM content, respectively.

Thermal conductivity of pristine PDMS is similar to the timber. Also, based on the graphs (Fig. 3), the HGM addition decreases TC in concentration dependent manner. Meanwhile, with the filler concentration up to 2.5 wt.%, more rapid decrease in TC is observed — by 39.8% for 2.5% HGM content. At the concentrations from 2.5 to 10 wt.% inverse relationship is observed also, but less significant. Minimal thermal conductivity was for 10 wt.% HGM-content and was 0.059 $W \cdot m^{-1} \cdot K^{-1}$, that is less by 57% than TC of the pristine PDMS. Modern thermal insulators, such as polystyrene foam and polyurethane aerogel, have a thermal conductivity of about 0.036 $W \cdot m^{-1} \cdot K^{-1}$ and 0.014 $W \cdot m^{-1} \cdot K^{-1}$, respectively. Thus, the thermal insulation properties of the resulting composite are inferior to these materials.

Result of thermal conductivity is different from the data obtained by Vlassov et al. [40], that achieved the decrease of thermal conductivity by 22% for 10 wt.% HGM-content. Possible reasons include the using of HGM from different manufacturer. Because of that, HGM in this work can be more mechanically resistant. Also, we used different mixing method — in the Vlassov's work solutions were mixed manually. The process of mixing has important role in this case, because HGM, destroying before curing, are not involved in the decreasing of the materials TC. This reason is also supported by a bigger decrease in TC in our works.

3.4. Mechanical properties

The results of the tensile tests and characteristic curves for the materials based on PDMS with various HGM concentration from 0 to 10% are presented in Fig. 4. The moduli of elasticity for the PDMS/HGM-0, PDMS/HGM-2, PDMS/HGM-5, and PDMS/HGM-10 samples were 0.685 ± 0.123 MPa, 1.253 ± 0.082 MPa, 1.614 ± 0.090 MPa, and 3.075 ± 0.401 MPa, respectively; elongations at break (relative) were 180.2% ± 49.5%, 112.3% ± 13.2%, 73.7% ± 17.5%, 56.0% ± 29.6% accordingly.

It should be noted that the modulus of elasticity of, for example, polyurethane aerogel is approximately 307 kPa, which is significantly less than that of the obtained samples. Thus, with the best thermal insulation properties, this material exhibits significantly worse mechanical properties. In Ref. [41], which also used PDMS and HGM, a material with a high modulus of elasticity and flexibility was developed for a composite with 7.5 wt.%. This is probably due to a more gentle mixing regime and chemical modification of the spheres; the formation of foam, in addition to the addition of HGM, in this case makes it possible to compensate for defects, which increases the cyclic strength of the material compared to that obtained in this work.

With the increase of HGM concentration in the composite, the stretchability of the material is significantly decreased. At an HGM concentration of 5 wt.%, the elongation at break is reduced by more than half. This embrittlement can be attributed to several mechanisms related to filler-matrix interactions. The rigid HGMs act as stress concentration points within the compliant PDMS matrix, initiating local microcracks under tensile load. Furthermore, the inherently brittleness of the glass microspheres limits the ductility of the composite system, as the matrix deformation is constrained by the non-deformable filler particles. The large spread of elongation at break values

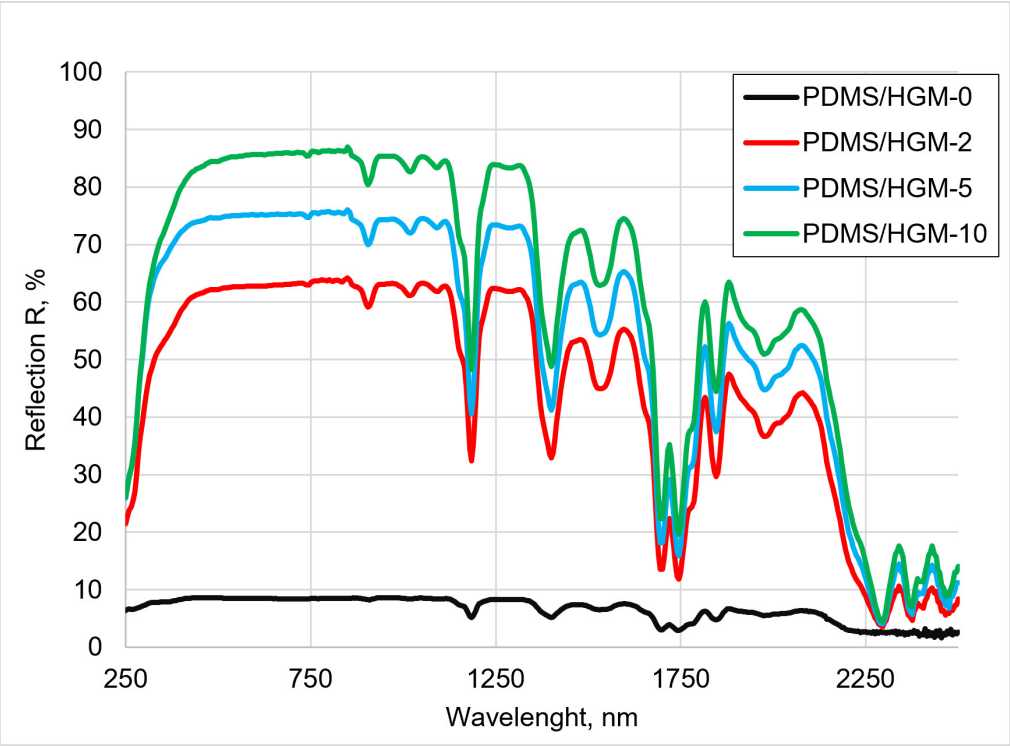

Fig. 5. Vis-NIR spectra of PDMS/HGM composite with 0% (black line), 2.5% (red line), 5% (blue line) and 10% (green line) HGM content.

indicates a possible dependence on the uniform distribution of HGM in the bulk of the composite (SEM images, Fig. 2e,f), which leads to a higher probability of forming defective zones in the material, such as cracks caused by HGM failure or delamination at the interface.

This analysis reveals a fundamental trade-off in PDMS/HGM composites between significantly enhanced thermal insulation properties and substantially reduced mechanical durability. The incorporation of HGM filler achieved a remarkable 57% reduction in thermal conductivity (to 0.059 $W \cdot m^{-1} \cdot K^{-1}$), making these composites competitive with conventional insulators like mineral wool, with the strong inverse correlation (–0.895) between HGM content and thermal conductivity enabling predictable material design. However, this improvement came at the expense of mechanical performance, manifested as severe embrittlement with elongation at break reduced by more than half at just 5 wt.% HGM due to stress concentration, constrained matrix deformation, interfacial failure, and filler fragmentation. The application-specific optimization of HGM concentration is therefore essential — lower loadings (2.5–5 wt.%) may suit applications requiring some flexibility, while higher loadings (up to 10 wt.%) are appropriate where thermal performance is prioritized over mechanical properties. Future research should focus on mitigating this trade-off through surface functionalization of HGMs to improve interfacial adhesion and potentially preserve both thermal and mechanical performance.

3.5. Optical properties measurement

The HGM filler significantly decreases the reflectivity of PDMS at any concentration (Fig. 5). The reflection of the composite with 2.5% HGM is 60% in the optical spectrum, which is 6 times higher than the value for pristine PDMS. However, the composite with 10% HGM demonstrates 85% reflection, showing a less pronounced increase in reflectance at higher concentrations. This optical behavior is primarily attributed to the intrinsic opacity of the glass microspheres and light scattering phenomena. As the HGM concentration rises, several mechanisms contribute to transparency loss: (1) increased light scattering at the polymer-filler interface due to the refractive index mismatch between PDMS (~1.43) and glass (~1.52); (2) the formation of microscopic agglomerates that act as additional light scattering centers; (3) potential void formation around imperfectly bonded filler particles; and (4) the cumulative effect of multiple scattering events from the numerous HGM surfaces throughout the material volume. The low density of the filler indeed leads to a large number of HGM particles in the material volume, explaining the transparency decrease even at low HGM concentrations (from 1.0 wt.%). Increasing the HGM concentration enchances the reflectivity of the material, but no shift in the peaks is observed, which indicates the absence of the formation of new chemical bonds in the material (Fig. 5). This combination of factors — particularly the dominant light scattering effects — excludes the possibility of using

the resulting composite as a basis for developing photocatalytically active porous materials where optical transparency is essential for photon penetration and catalytic activation.

3.6. Surface properties

For the composite materials based on PDMS with the addition of HGM (not less than 1.0%), the work of adhesion drops sharply below the detection limit ($< 16 \cdot 10^{-5}$ J·m^{-2}). Work of the adhesion for the pristine PDMS is $28 \cdot 10^{-2}$ J·m^{-2}. Hence, it can be concluded that the addition of microspheres significantly affects the surface properties of the material.

A number of possible reasons can explain the results obtained. This effect may be due to the weak adhesive interaction of the hollow glass microspheres of the filler with the glass probe and the occupancy of the chemical bonds of the polymer by the surface of the hollow glass microspheres. In common case, mainly the terminated and radical groups (branches) of polymers chain can be involved in adhesion interactions. Another reason is surface roughness. Surface of composite materials (with HGM) is less smooth than the pristine material. This fact is indirectly confirmed by the variations of wetting angles values. For the composite with 10% content filler the deviation more widely than for the pristine materials. High surface roughness has an inverse effect on the real contact area under conditions of low contact pressure and short loading time [44,45]. The small real contact area leads to the decrease of adhesion between two materials. However, for the work of adhesion to decrease by three orders of magnitude (as observed in this study), the surface roughness would have to be very high, and the variation in the contact angle would have to be significantly greater than what we observed. Summary, all factors influence in the decreasing work of adhesion for the composites with HGM from 1% content filler.

The equilibrium contact angle between water drop and top surface of PDMS/HGM-10 composite is 100.0±9.7°, that is significantly larger than angle of PDMS/HGM-0 composite's surface (74.4±3.6°).

4. CONCLUSIONS

This study successfully demonstrates the feasibility of developing PDMS-based composite materials with hollow glass microspheres for thermal insulation applications. The experimental results provide a clear justification for this approach: we achieved a significant reduction in thermal conductivity — up to 57% compared to pristine PDMS — reaching values as low as 0.059 W·m^{-1}·K^{-1}, which is competitive with conventional insulation materials like mineral wool, almost twice times less than polystyrene foam (0.036 W·m^{-1}·K^{-1}) and half an order of magnitude less than polyurethane aerogel (0.014 W·m^{-1}·K^{-1}), which is compensated by a large modulus of elasticity. This enhancement is attributed to the introduction of pseudo-porosity via HGM incorporation and the effective degassing procedure, which eliminates air bubbles. Furthermore, the composites showed increased hardness, and critically, SEM analysis confirmed that the structural integrity of the insulating voids remains intact even after filler destruction, ensuring long-term stability of thermal properties under mechanical deformation.

However, the methodology employed – mechanical mixing and thermal curing with mold rotation – proved suboptimal for achieving uniform filler dispersion, as indicated by considerable scatter in mechanical property data. This heterogeneity currently limits the mechanical reliability of the composites, particularly their elongation at break.

ACKNOWLEDGEMENT

This work was supported by the Ministry of Science and Higher Education of the Russian Federation, project no. FSER-2025-0005.

REFERENCES

[1] M. Bäker, T. Fiedler, J. Rösler. Stress evolution in thermal barrier coatings for rocket engine applications. *Mechanics of Advanced Materials and Modern Processes*, 2015, vol. 1, no. 1, art. no. 5.

[2] K. Ersoy. Review of electronic cooling and thermal management in space and aerospace applications. *Engineering Proceedings,* 2025, vol. 89, no. 1, art. no. 42.

[3] S. Zhu, X. Li, Z. Luo, X. Jia, Y. Qin, H. Guo, J. Tang, Z. Li, H. Wen, Z. Ma, J. Liu. A two-stage insulation method for suppressing thermal crosstalk in microarray sensitive units. *Applied Physics Express*, 2024, vol. 17, no. 3, art. no. 037001.

[4] M.K. Sharma, B. Ramos-Alvarado. Thermal management of 3-D heterogeneously integrated microelectronics: Challenges and future research directions. *Communications Engineering*, 2026, vol. 5, no. 1, art. no. 28.

[5] G. Gilardi, W. Yao, H. Rabbani Haghighi, X.J.M. Leijtens, M.K. Smit, M.J. Wale. Deep trenches for thermal crosstalk reduction in InP-based photonic integrated circuits. *Journal of Lightwave Technology*, 2014, vol. 32, no. 24, pp. 4864–4870.

[6] G. Previati, G. Mastinu, M. Gobbi. Thermal management of electrified vehicles—A review. *Energies*, 2022, vol. 15, no. 4, art. no. 1326.

[7] H.M. Kim, Y.J. Noh, J. Yu, S.Y. Kim, J.R. Youn. Silica aerogel/polyvinyl alcohol (PVA) insulation composites with preserved aerogel pores using interfaces between the superhydrophobic aerogel and hydrophilic PVA solution. *Composites Part A: Applied Science and Manufacturing*, 2015, vol. 75, pp. 39–45.

[8] D. Ge, L. Yang, Y. Li, J. Zhao. Hydrophobic and thermal insulation properties of silica aerogel/epoxy composite.

Journal of Non-Crystalline Solids, 2009, vol. 355, no. 52–54, pp. 2610–2615.

[9] S.Y. Kim, Y.J. Noh, J. Lim, N.-H. You. Silica aerogel/polyimide composites with preserved aerogel pores using multi-step curing. *Macromolecular Research*, 2014, vol. 22, no. 1, pp. 108–111.

[10] H.M. Kim, H.S. Kim, S.Y. Kim, J.R. Youn. Silica aerogel/epoxy composites with preserved aerogel pores and low thermal conductivity. *e-Polymers*, 2015, vol. 15, no. 2, pp. 111–117.

[11] K. Li, Y. Wang, X. Zhang, J. Wu, X. Wang, A. Zhang. Intrinsically hydrophobic magnesium oxychloride cement foam for thermal insulation material. *Construction and Building Materials*, 2021, vol. 288, art. no. 123129.

[12] C.-K. Jeon, J.-S. Lee, H. Chung, J.-H. Kim, J.-P. Park. A study on insulation characteristics of glass wool and mineral wool coated with a polysiloxane agent. *Advances in Materials Science and Engineering*, 2017, vol. 2017, art. no. 3938965.

[13] X. Guo, J. Feng. Facilely prepare passive thermal management materials by foaming phase change materials to achieve long-duration thermal insulation performance. *Composites Part B: Engineering*, 2022, vol. 245, art. no. 110203.

[14] J. Zou, S. Li, Z. Yuan, X. Pei, H. Yu, P. Chen, D. Ye. Temperature-mediated construction of a plantar pressure-relieving, thermally insulating, and biodegradable thick-walled cellulose sponge insole. *Chemical Engineering Journal*, 2023, vol. 451, art. no. 138876.

[15] M. Vahtrus, S. Oras, M. Antsov, V. Reedo, U. Mäeorg, A. Lõhmus, K. Saal, R. Lõhmus. Mechanical and thermal properties of epoxy composite thermal insulators filled with silica aerogel and hollow glass microspheres. *Proceedings of the Estonian Academy of Sciences*, 2017, vol. 66, no. 4, pp. 339–346.

[16] Y. Sun, Y. Chu, C. Deng, H. Xiao, W. Wu. High-strength and superamphiphobic chitosan-based aerogels for thermal insulation and flame retardant applications. *Colloids and Surfaces A: Physicochemical and Engineering Aspects*, 2022, vol. 651, art. no. 129663.

[17] C. Zhang, L. Qu, Y. Wang, T. Xu, C. Zhang. Thermal insulation and stability of polysiloxane foams containing hydroxyl-terminated polydimethylsiloxanes. *RSC Advances*, 2018, vol. 8, no. 18, pp. 9901–9909.

[18] Z.A. Abd Halim, N. Ahmad, M.A.M. Yajid, H. Hamdan. Thermal insulation performance of silicone rubber / silica aerogel composite. *Materials Chemistry and Physics*, 2022, vol. 276, art. no. 125359.

[19] J. Ren, X. Huang, J. Shi, W. Wang, J. Li, Y. Zhang, H. Chen, R. Han, G. Chen, Q. Li, Z. Zhou. Transparent, robust, and machinable hybrid silica aerogel with a "rigid-flexible" combined structure for thermal insulation, oil/water separation, and self-cleaning. *Journal of Colloid and Interface Science*, 2022, vol. 623, pp. 1101–1110.

[20] M.L. Hammock, A. Chortos, B.C.-K. Tee, J.B.-H. Tok, Z. Bao. 25th Anniversary article: The evolution of electronic skin (E-skin): A brief history, design considerations, and recent progress. *Advanced Materials*, 2013, vol. 25, no. 42, pp. 5997–6038.

[21] S. Torino, B. Corrado, M. Iodice, G. Coppola. PDMS-based microfluidic devices for cell culture. *Inventions*, 2018, vol. 3, no. 3, art. no. 65.

[22] C. Majidi. Soft robotics: A perspective—Current trends and prospects for the future. *Soft Robotics*, 2014, vol. 1, no. 1, pp. 5–11.

[23] I.M. Sosnin, S. Vlassov, L.M. Dorogin. Application of polydimethylsiloxane in photocatalyst composite materials: A review. *Reactive and Functional Polymers*, 2021, vol. 158, art. no. 104781.

[24] M. Taha, A. Khalid, M.G. Elmahgary, S.S. Medany, Y.A. Attia. Fabricating a 3D floating porous PDMS − Ag/AgBr decorated g-C_3N_4 nanocomposite sponge as a re-usable visible light photocatalyst. *Scientific Reports*, 2024, vol. 14, no. 1, art. no. 4184.

[25] J.-Y. Kim, K.-S. Jang. Facile fabrication of stretchable electrodes by sedimentation of Ag nanoparticles in PDMS matrix. *Journal of Nanomaterials*, 2018, vol. 2018, art. no. 4580921.

[26] L. Chen, C. Ma, L. Li, C. Zhu, J. Gu, H. Gao, Z. Zhu, C. Du, T. Wang, J. Xu, G. Chen. Using PDMS plasma cavity SERS substrate for the detection of aspartame. *Journal of Spectroscopy*, 2020, vol. 2020, art. no. 4212787.

[27] M.P. Wolf, G.B. Salieb-Beugelaar, P. Hunziker. PDMS with designer functionalities—Properties, modifications strategies, and applications. *Progress in Polymer Science*, 2018, vol. 83, pp. 97–134.

[28] D. Cambié, C. Bottecchia, N.J.W. Straathof, V. Hessel, T. Noël. Applications of continuous-flow photochemistry in organic synthesis, material science, and water treatment. *Chemical Reviews*, 2016, vol. 116, no. 17, pp. 10276–10341.

[29] S. Ling, W. Chen, Y. Fan, K. Zheng, K. Jin, H. Yu, M.J. Buehler, D.L. Kaplan. Biopolymer nanofibrils: Structure, modeling, preparation, and applications. *Progress in Polymer Science*, 2018, vol. 85, pp. 1–56.

[30] Z. Chen, G. Cheng, Y. Zhu, H. Wu, E. Dong, P. Gu, Y. Zhao. Biomimetic polydimethylsiloxane (PDMS)/carbon fiber lamellar adhesive composite in thermal vacuum environment. *International Journal of Adhesion and Adhesives*, 2021, vol. 105, art. no. 102778.

[31] Z. Xie, Y. Cai, Z. Wei, Y. Zhan, Y. Meng, Y. Li, Y. Li, Q. Xie, H. Xia. Robust and self-healing polydimethylsiloxane/carbon nanotube foams for electromagnetic interference shielding and thermal insulation. *Composites Communications*, 2022, vol. 35, art. no. 101323.

[32] N. Al-Khudary, P.Y. Cresson, Y. Orlic, P. Coquet, P. Pernod, T. Lasri. Measurement of the thermal conductivity of polydimethylsiloxane polymer using the three omega method. *Key Engineering Materials*, 2014, vol. 613, pp. 259–266.

[33] J.-H. Hao, Q. Chen, K. Hu. Porosity distribution optimization of insulation materials by the variational method. *International Journal of Heat and Mass Transfer*, 2016, vol. 92, pp. 1–7.

[34] T. Zhao, Y. Yu, Y. Zhang, Z. Lyu, C. Li, D. Hu, Q. Li. Lightweight and dual-functional composites with stiff-soft microstructure for energy absorption and thermal insulation. *Composites Communications*, 2021, vol. 26, art. no. 100778.

[35] H. Lee, D. Lee, J. Cho, Y.-O. Kim, S. Lim, S. Youn, Y.C. Jung, S.Y. Kim, D.G. Seong. Super-insulating, flame-retardant, and flexible poly(dimethylsiloxane) composites based on silica aerogel. *Composites Part A: Applied Science and Manufacturing*, 2019, vol. 123, pp. 108–113.

[36] M. Timusk, I.A. Nigol, S. Vlassov, S. Oras, T. Kangur, A. Linarts, A. Šutka. Low-density PDMS foams by controlled destabilization of thixotropic emulsions. *Journal of Colloid and Interface Science*, 2022, vol. 626, pp. 265–275.

[37] I.-L. Ngo, S. Jeon, C. Byon. Thermal conductivity of transparent and flexible polymers containing fillers: A literature review. *International Journal of Heat and Mass Transfer*, 2016, vol. 98, pp. 219–226.
[38] A. Trofimov, L. Pleshkov, H. Back. Hollow glass microspheres for high strength composite cores. *Reinforced Plastics*, 2006, vol. 50, no. 7, pp. 44–46, 48–50.
[39] E.V. Antonov, I.M. Sosnin, S. Vlassov, L.M. Dorogin. Polydimethylsiloxane/glass-based composite elastomer for thermophysical applications. *Reviews on Advanced Materials and Technologies*, 2022, vol. 4, no. 1, pp. 28–32.
[40] S. Vlassov, S. Oras, M. Timusk, V. Zadin, T. Tiirats, I.M. Sosnin, R. Lõhmus, A. Linarts, A. Kyritsakis, L.M. Dorogin. Thermal, mechanical, and acoustic properties of polydimethylsiloxane filled with hollow glass microspheres. *Materials*, 2022, vol. 15, no. 5, art. no. 1652.
[41] T.-L. Han, B.-F. Guo, G.-D. Zhang, L.-C. Tang. Facile synthesis of hollow glass microsphere filled PDMS foam composites with exceptional lightweight, mechanical flexibility, and thermal insulating property. *Molecules*, 2023, vol. 28, no. 6, art. no. 2614.
[42] L. Dorogin, B.N.J. Persson. Contact mechanics for polydimethylsiloxane: From liquid to solid. *Soft Matter*, 2018, vol. 14, no. 7, pp. 1142–1148.
[43] R. Tadmor. Line energy and the relation between advancing, receding, and Young contact angles. *Langmuir*, 2004, vol. 20, no. 18, pp. 7659–7664.
[44] A. Tiwari, L. Dorogin, A.I. Bennett, K.D. Schulze, W.G. Sawyer, M. Tahir, G. Heinrich, B.N.J. Persson. The effect of surface roughness and viscoelasticity on rubber adhesion. *Soft Matter*, 2017, vol. 13, no. 19, pp. 3602–3621.
[45] L. Dorogin, A. Tiwari, C. Rotella, P. Mangiagalli, B.N.J. Persson. Adhesion between rubber and glass in dry and lubricated condition. *Journal of Chemical Physics*, 2018, vol. 148, no. 23, art. no. 234702.

УДК 620.22:538.9

Полидиметилсилоксановый теплоизоляционный композитный эластомер, наполненный полыми стеклянными микросферами

Е.В. Антонов [1], D. Castro [2], П.П. Снетков [1], С.Н. Морозкина [1,3], И.М. Соснин [1,4], Л.М. Дорогин [1]

[1] Институт перспективных систем передачи данных, Университет ИТМО, Кронверкский пр., 49, лит. А, СПб, 197101, Россия
[2] Центр химической инженерии, Университет ИТМО, Кронверкский пр., 49, лит. А, СПб, 197101, Россия
[3] Кабардино-Балкарский государственный университет, ул. Чернышевского, 174, Нальчик, Россия
[4] Тольяттинский государственный университет, ул. Белорусская, 14, Тольятти, 445020, Россия

Аннотация. Данная работа посвящена улучшению теплоизоляционных свойств полидиметилсилоксана путем введения полых стеклянных микросфер в качестве функционального наполнителя, а также оценка оптимальных механических, поверхностных и оптических характеристик. Были исследованы теплопроводность, механические свойства при растяжении, характеристики поверхности и оптическая прозрачность композитов. Введение 10 мас.% полых стеклянных микросфер снизило коэффициент теплопроводности на 56,3%, достигнув минимального значения 0,059 Вт·м$^{-1}$·К$^{-1}$. Однако это улучшение было достигнуто за счет оптической прозрачности, свойств поверхности и значительного снижения критического относительного удлинения. Результаты показывают, что композит на основе полидиметилсилоксана, наполненный полыми стеклянными микросферами, являются перспективными материалами для применения в качестве теплоизолятора, где прозрачность и растяжимость являются вторичными по отношению к тепловым характеристикам.

Ключевые слова: теплопроводность; микросферы; адгезия; полидиметилсилоксан; композиционный материал